

NASA TN D-890

NASA TN D-890



TECHNICAL NOTE

D-890

SIMPLE FORMULAS FOR STAGNATION-POINT CONVECTIVE
HEAT LOADS IN LUNAR RETURN

By Frederick C. Grant

Langley Research Center
Langley Field, Va.

NATIONAL AERONAUTICS AND SPACE ADMINISTRATION
WASHINGTON

July 1961



NATIONAL AERONAUTICS AND SPACE ADMINISTRATION

TECHNICAL NOTE D-890

SIMPLE FORMULAS FOR STAGNATION-POINT CONVECTIVE

HEAT LOADS IN LUNAR RETURN

By Frederick C. Grant

SUMMARY

L
1
6
1
5

Simple formulas are given for the stagnation-point convective heat loads in lunar return for two operational modes. The two modes of operation analyzed are typical of moderate heating and of nearly minimum heat loads, respectively. The values of the parameters in a simple two-parameter formula for the total-heat load are given in the lift-drag-ratio range of 0.2 to 1.0 and in the peak loading range of 2g to 10g. For vehicles having a lift-drag ratio near 0.5, which is typical of many proposed lunar return vehicles, the nominal mode had about 20 percent more absorption than the nearly minimum mode.

INTRODUCTION

In the course of preliminary trajectory analysis of the lunar return problem it was found possible to compress a large amount of stagnation-point heating data into simple formulas for a range of vehicle lift-drag ratios and a range of peak loadings which are of current interest for manned vehicles. Several modes of operation which span a range of heat loads are considered.

SYMBOLS

A	reference area, sq ft
c	satellite speed at altitude of 50 miles, 25,800 ft/sec
C_D	drag coefficient
$C_{\dot{q}}$	constant in heating-rate formula
D	drag

2

$$G = \frac{R}{W}$$

g acceleration due to gravity, 32.2 #t/sec²

h altitude, ft

L lift

n exponent in heating-rate formula

Q heat absorbed per unit area at stagnation point, Btu/sq ft

\dot{q} heating rate per unit area at stagnation point, Btu/sq ft-sec

R resultant force

r radius of curvature, ft

s longitudinal range, ft

t time, sec

$$u = \frac{V}{c}$$

V airspeed, ft/sec

W weight, lb

β^{-1} scale height, 24,500 ft

γ flight-path angle, deg

$$\delta = \frac{W}{C_D A r}, \text{ lb/cu ft}$$

ρ air density, slugs/cu ft

ϕ roll angle, deg

Subscripts:

l start of constant-altitude segment

l' start of constant-G segment

L
1
6
1
5

2 end of constant-altitude segment

2' end of constant-G segment

Dot over symbol indicates differentiation with respect to time.

PARAMETER RANGES

L The parameter range considered is indicated in figure 1 in terms
 1 of Chapman's corridor width. (See ref. 1.) Corridor width is a meas-
 6 ure of the error in perigee height of the approach orbit which is per-
 1 missible for a given load limit. Fixed angle of attack and fixed
 5 geometry are assumed in figure 1. Consideration of guidance accuracy,
 atmospheric density variations, and piloting errors will fix the cor-
 ridor width. Since the gross weight of the vehicle tends to increase
 with $(L/D)_{\max}$ capability, the lightest vehicle will have the lowest
 $(L/D)_{\max}$ capability consistent with the constraints of load limits,
 corridor width, and maneuver capability. If a load limit of $10g$ and
 a corridor width of 50 miles are adopted as extreme values, the high
 values of L/D need not be considered. Accordingly, attention has
 been restricted to values of L/D less than one. Simple formulas were
 not found below $L/D = 0.2$ so smaller values than 0.2 are not included.
 If a lower load limit such as $5g$ is adopted (see fig. 1), it should be
 noted that some minimum value of $(L/D)_{\max}$ is required to meet the load
 limit even with perfect guidance (zero corridor).

In short, small corridor widths allow low values of L/D , and
 small load limits force high values of L/D . Corridor width is inde-
 pendent of $W/C_D A$ so vehicle weight does not appear in figure 1. The
 parameter range of $25 \leq W/C_D A \leq 400$ lb/sq ft was adopted in the cal-
 culations to span a wide range of weights.

MODES OF OPERATION

The aerodynamic coefficients are not allowed to vary in the modes
 of operation considered. The values of L/D and δ are thus fixed
 through each entry. Control is exercised by rolling the vehicle (and
 thus the lift) about the velocity vector. In general, a discontinuous
 jump in roll angle followed by a continuous variation is required.
 Formulas defining the required roll-angle variations are given in
 appendixes A and B.

Constant G

A convenient lower bound for the total-heat load to be experienced in lunar return is provided by what will be called a constant-G ($dG = 0$) entry. In this entry (see fig. 2) the vehicle makes a constant roll-angle ($d\phi = 0$) pull-up to the point of peak G. At this point a sudden roll is presumed which is followed by a continuous roll in such a manner as to keep the aerodynamic loading constant. The constant-G entry maintains during the slow-up the highest Reynolds number consistent with the load limit and hence the lowest ratio of friction to pressure drag. If the constant-G flight is presumed to continue to zero velocity, a lower bound to the heat absorption is established. The speed to which constant G can actually be maintained (see appendix A) is near enough to zero in the parameter range of interest that the bound obtained cannot differ greatly from the sharper bound obtained in an entry with a dynamically possible low-speed portion.

L
1
6
1
5

Constant h

A second mode considered is the constant-altitude ($dh = 0$) slow-up. This mode is believed to yield heat loads more typical of actual one-pass entries than the quasi-limiting case of constant loading. In the constant-altitude mode a constant roll-angle ($d\phi = 0$) pull-up is followed by the constant-altitude slow-up, which is followed by a smooth glide to impact. (See appendix B.) As in the previous case, a continuous roll is presumed as the control technique. The mode is characterized by sustained but steadily decreasing loads through most of the entry.

Constant ϕ

A third mode considered was the fixed-control ($d\phi = 0$) mode. Results are given only for $L/D = 0.5$ which is typical of many proposed lunar return vehicles. This mode is objectionable for reasons other than higher heating, but it is introduced to provide a measure for a relatively high total-heating mode somewhat as an upper bound to complement the lower bound provided by the constant-G mode. Of course, the constant- ϕ mode is not an absolute upper bound.

POWER LAWS

Examination of the trajectory data obtained in the parameter range of figure 1 has indicated that, for the modes of operation considered, the peak heating rate at the stagnation point during entry is

$$\dot{q}_{\max} = K_{\dot{q}} \sqrt{\delta G}^y \quad (1a)$$

and the total heat absorbed at the stagnation point during entry is

$$Q = K_Q \sqrt{\delta G}^{-x} \quad (1b)$$

for $\delta = W/C_D A r$. The values of the constants K_Q , $K_{\dot{q}}$, x , and y were obtained from plots similar to the sample shown as figure 3. The scatter of the data is typical of that observed in the range, $0.2 \leq L/D \leq 1.0$, and in the range, $25 \leq \delta r \leq 400$ lb/sq ft. Just as in figure 3 the slope of the line fixes x and the vertical position fixes K_Q , so do the slope and vertical position fix the exponents and constants in all cases. The values of K_Q , $K_{\dot{q}}$, x , and y depend, of course, on the mode of operation and the operating L/D . These values are shown in figures 4 and 5 for two modes of operation. In reference 1 somewhat more complex relations than those of equations (1a) and (1b) are suggested, and the corresponding constants are evaluated for a number of modes of operation.

Much of the data was taken from numerical integrations performed by an IBM 7090 electronic data processing system. Some analytical calculations were made as outlined in appendixes A and B. The stagnation-point, convective-heating-rate formula used throughout was of the type used in reference 2 and is as follows:

$$\dot{q} = 17,300 \sqrt{\rho} \left(\frac{V}{10^4} \right)^{3.15} \text{ Btu/sq ft-sec}$$

where ρ is in slugs/cu ft, V is in feet per second, and a radius of curvature of 1 foot is assumed. The assumed initial conditions in every case were $V = 36,500$ ft/sec at $h = 400,000$ ft in a static, radially symmetric ARDC 1959 atmosphere. (See ref. 3.) In the analytical calculations, an exponential atmospheric density variation with altitude is used.

RESULTS AND DISCUSSION OF TYPICAL VEHICLE

Equations (1a) and (1b) yield an interesting result when applied to vehicles having a lift-drag ratio of 0.5 which is typical of many proposed lunar return vehicles. Total-heat loads at the stagnation point of these vehicles are shown in figure 6 for a range of G_{\max}

from 2 to 10. Only entries for positive lift in the pull-up are shown in figure 6. Limiting cases for negative lift in the pull-up are shown subsequently.

With the assumption that the values of $Q/\sqrt{\delta}$ for the constant-altitude mode are representative of likely levels of heat absorption, figure 6 shows a rather small improvement to be found by resorting to the constant-G mode and a similar small penalty for the change to the constant- ϕ mode. In each case the change in heat absorption is about 20 percent.

The range in heat loads for a given mode is of interest when entries high and low in the entry corridor are considered. Figure 6 represents undershot entries in the sense that for each level of G_{\max} the steepest entry has been made within the constraint of constant coefficients. The steepest entry is assured because upward lift is used in the entire pull-up. The overshoot boundary may be defined by an entry in which use of downward lift through the initial pull-up just insures that the vehicle will not skip. After this marginal pull-up the vehicle may maneuver to lower altitudes and make an upright pull-up followed by one of the previously discussed modes of operation. An illustrative case is shown in figure 7 again for the constant-h and constant-G modes at $L/D = 0.55$. Some description of the complicated modes of operation corresponding to the overshoot boundary curves in figure 7 is necessary. The vehicle enters the atmosphere with the lift vector in a vertical plane pointing downward. The entry is so shallow that when the vehicle levels out there is just enough lift to overcome the resultant of the centrifugal force and the weight. Since this resultant is decreasing faster than the lift, the vehicle bites deeper into the atmosphere in an inverted attitude. By rolling to a normal upright attitude at increasingly later times the vehicle may make pull-ups at increasingly higher values of G followed by the usual slow-up phases of the constant-h and constant-G modes. The heat absorption indicated as overshoot values in figure 7 corresponds to entries made in this manner. It is apparent from the figure that the penalty for overshoot entries within a given mode increases with the loading level of the entry, reaching appreciable values (larger than 20 percent) at the higher-loading levels. It was not found possible to accurately represent entries of the type considered in figure 7 by formulas similar to equations (1a) and (1b).

Of course, it should be remembered that all results refer to the convective component of the heat load. Inclusion of the radiative component would add to the values shown.

CONCLUDING REMARKS

Simple relations have been given for the stagnation-point convective heat loads in lunar return for two operational modes. About 20 percent more heat absorption was found for a nominal mode typical of one-pass sustained loading entries (constant altitude) than for a mode with nearly minimum absorption (constant loading). For vehicles having a lift-drag ratio near 0.5, operation with fixed controls resulted in total heat loads 20 percent higher than those experienced in the constant-altitude mode.

L
1
6
1
5

Langley Research Center,
National Aeronautics and Space Administration,
Langley Field, Va., June 9, 1961.

APPENDIX A

CONSTANT-G MODE

The limiting case of constant G , so-called, can be easily handled analytically for the constant-trim, variable-roll mode of control. Constant trim implies nearly constant aerodynamic coefficients in the hypersonic speed range so that constant dynamic pressure is required for a constant-loading level. Thus,

$$G = \frac{R}{W} = \sqrt{1 + \left(\frac{L}{D}\right)^2} \frac{\rho V^2}{2\delta r} = \text{Constant} \quad (\text{A1})$$

The trajectory profile is sketched in figure 2. The condition that $dG = 0$ may be written as follows:

$$\frac{d}{dt}(\rho V^2) = \dot{\rho} V^2 + 2\rho V \dot{V} = 0 \quad (\text{A2})$$

Assuming an exponential atmosphere and neglecting gravity-induced speed changes gives

$$\dot{\rho} = -\beta \rho V \sin \gamma \quad (\text{A3a})$$

$$-\dot{V} = \frac{D}{W} g \quad (\text{A3b})$$

Upon combining equation (A2) with (A3), introducing $\dot{s} = V \cos \gamma$, and integrating, the distance traveled on 1-2' (see fig. 2) is found as

$$\beta s_{1,2'} = -\tan^{-1} \sqrt{\frac{V_{1'}^4 \beta^2}{4\left(\frac{D}{W}\right)^2 g^2} - 1} + \sqrt{\frac{V_{1'}^4 \beta^2}{4\left(\frac{D}{W}\right)^2 g^2} - 1} \quad (\text{A4a})$$

Equation (A4a) assumes the constant deceleration to be maintained to zero velocity, which is incorrect but introduces only a small error. For the large values of $V_{1'}$, which are of concern in lunar return,

$$s_{1,2'} \approx \frac{V_{1'}^2}{2 \frac{D}{W} g} \quad (\text{A4b})$$

which is just the result to be found by assuming $\gamma = 0$ through the deceleration period. This result implies that γ remains small through most of the arc 1'2'.

The question of just how long the constant deceleration can actually be maintained is of interest. On 1'2' the required flight-path angle can be found from equations (A2) and (A3) as

$$\sin \gamma = - \frac{g}{\beta \delta r} \rho \quad (\text{A5a})$$

or as

$$\sin \gamma = - \frac{2gG}{c^2 \beta} \frac{u^{-2}}{\sqrt{1 + \left(\frac{L}{D}\right)^2}} \quad (\text{A5b})$$

Since γ is small and remains small except in the neighborhood of point 2',

$$\cos \gamma \dot{\gamma} \approx \dot{\gamma} \approx - \frac{g}{\beta \delta r} \rho \quad (\text{A6})$$

is the required rate of change of flight-path angle. Equation (A6) is assumed to be satisfied by rotation of the lift vector about the velocity vector in a slow continuous roll. The governing equation for γ is

$$\frac{V}{g} \dot{\gamma} = \frac{L}{W} \cos \phi + (u^2 - 1) \cos \gamma \quad (\text{A7})$$

The value of ϕ is to be varied in the manner required to satisfy equation (A7) since it is the only quantity not fixed by the constraint of constant G . The condition $\cos \phi = -1$ defines point 2', the place beyond which constant G cannot be maintained. At point 2' the lift vector is pointing downward in the vertical plane. Conditions at point 2' are defined by combining equations (A3a), (A6), and (A7) into the following relation:

$$2 \frac{D}{W} \tan \gamma_{2'} + \frac{L}{W} = (u_{2'}^2 - 1) \cos \gamma_{2'} \quad (\text{A8a})$$

This transcendental equation for $\gamma_{2'}$ has supercircular and sub-circular solutions. The subcircular solution corresponds to point 2'.

L
1
6
1
5

A convenient approximate solution to equation (A8a) exists when $u_{2'}^2 \ll 1$ and $\cos \gamma_{2'} \approx 1$ as

$$-\tan \gamma_{2'} = \frac{1}{2} \left[\frac{L}{D} + \frac{1}{G} \sqrt{1 + \left(\frac{L}{D} \right)^2} \right] \quad (\text{A8b})$$

Precise solutions to equation (A8a) are shown in figure 8. The case of low values of L/D and high values of G will yield a measure of the smallest velocity range through which constant G can be maintained. Figure 8 shows that, for $L/D = 0.2$ and $G_{\max} = 10$, $-\gamma_{2'} = 8.2^\circ$ at $u_{2'} = 0.4$. Even in this unfavorable case the fraction of satellite-speed kinetic energy remaining at point 2' is small.

L
1
6
1
5

If stagnation-point total heat absorbed is calculated on the basis of uniform deceleration through the velocity range from u_1 to zero, then

$$Q_{1,2'} = \frac{C_{\dot{q}}}{g} \sqrt{\frac{2\delta}{D/W}} \frac{V_{1'}^n}{n} \quad (\text{A9})$$

when

$$\dot{q} = C_{\dot{q}} \sqrt{\rho} V^n$$

The heat loads absorbed in the slow-up for the case of $dG = 0$ in figures 6 and 7 were computed with the use of equation (A9) which assumes constant deceleration to zero velocity. The previous calculation of $u_{2'}$ shows that $u_{2'}^2$ is always small for $L/D \geq 0.2$ and $G \leq 10$. The conclusion to be drawn is that the values of Q in figure 6 are lower than those experienced in an entry with a dynamically possible low-speed portion. The values of Q yield a lower bound but not a greatest lower bound. However, the neglected contributions to Q appear to be small enough so that the lower bound provided by the constant- G mode is not far from a greatest lower bound for the constant-trim, rolling-control mode of operation.

APPENDIX B

CONSTANT-ALTITUDE MODE

The calculations of the characteristics of this mode of entry assume that the altitude control is a continuous roll about the velocity vector. The governing equation on the level flight portion is thus

$$0 = \frac{L}{W} \cos \phi + (u^2 - 1) \quad (B1)$$

which is the same as equation (A7) with $\dot{\gamma}$ set to zero. A limiting condition in this mode of entry occurs when $\cos \phi = -1$ is required at the bottom of the first pull-up. A necessary condition at the bottom of the first pull-up is the following inequality:

$$\left(\frac{L}{W}\right)_1 \geq u_1^2 - 1 \quad (B2)$$

For shallower entries than those for which (B2) is satisfied, a constant-altitude portion cannot be continued beyond point 1. In fact, there is a sharp but continuous transition in a narrow entry-angle range between high-apogee, long-range, skipping entries and those that satisfy inequality (B2).

Although the constant-altitude mode is merely illustrative of one-pass sustained loading entries, the assumed rolling mode of control has a more general interest. No changes in longitudinal trim and hence no aerodynamic pitch controls are required. Of course, the changes in heading angle and the buildup of lateral displacement caused by the left-over horizontal component of the lift complicate the guidance problem.

The elementary integrals of the motion along the constant-altitude arc 12 are as follows:

$$s_{12} = \frac{2\delta r}{\rho_1 g} \log_e \left(\frac{u_1}{u_2} \right) \quad (B3a)$$

$$t_{12} = \frac{cu_1}{\left(\frac{D}{W}\right)_g} \left(\frac{u_1}{u_2} - 1 \right) \quad (B3b)$$

$$Q_{12} = \frac{C_q \sqrt{\rho_1} c^{n+1}}{\left(\frac{D}{W}\right)_1 g} \frac{u_1^{n+1} - u_2^{n+1}}{n+1} \quad (\text{B3c})$$

where

$$\frac{1}{u_2} = \sqrt{1 + \frac{L}{D} \frac{\rho_1 c^2}{2\delta r}}$$

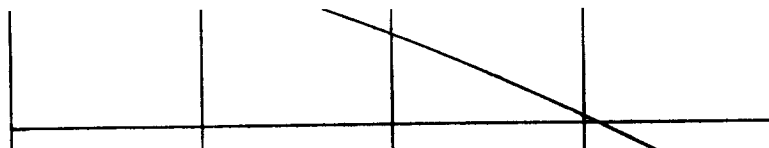
at the start of the smooth glide.

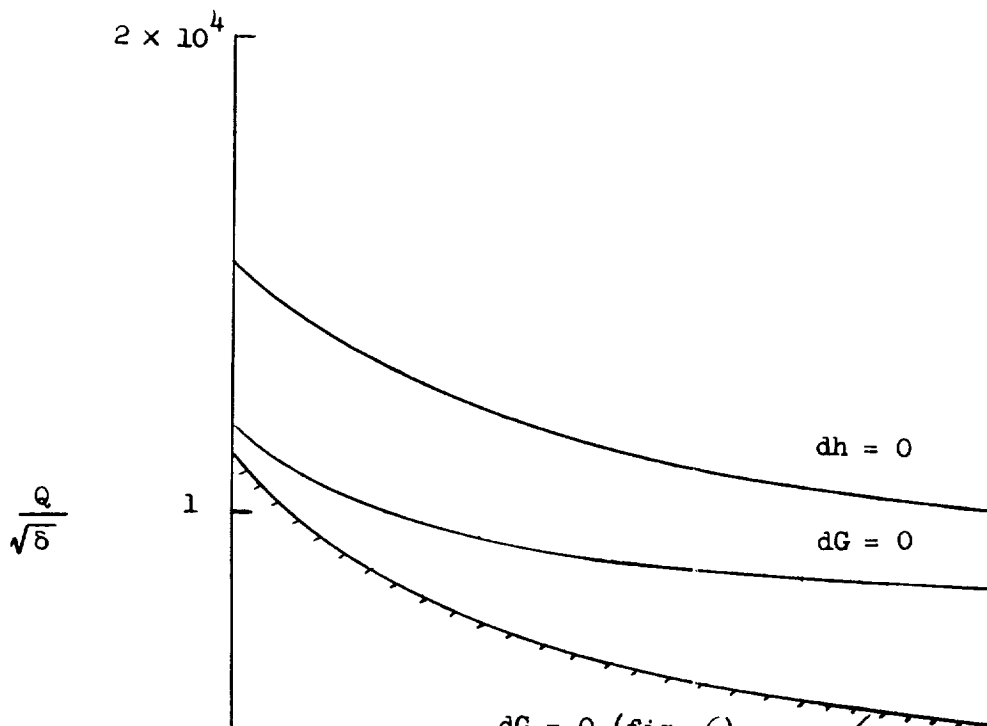
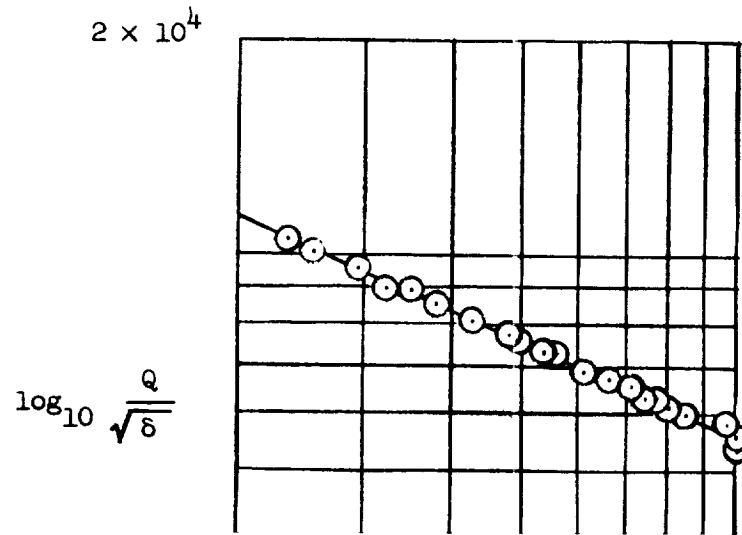
L
1
6
1
5

REFERENCES

1. Chapman, Dean R.: An Analysis of the Corridor and Guidance Requirements for Supercircular Entry Into Planetary Atmospheres. NASA TR R-55, 1960.
2. Detra, R. W., Kemp, N. H., and Riddell, F. R.: Addendum to 'Heat Transfer to Satellite Vehicles Re-entering the Atmosphere.' Jet Propulsion, vol. 27, no. 12, Dec. 1957, pp. 1256-1257.
3. Minzner, R. A., Champion, K. S. W., and Pond, H. L.: The ARDC Model Atmosphere, 1959. Air Force Surveys in Geophysics No. 115 (AFCRC-TR-59-267), Air Force Cambridge Res. Center, Aug. 1959.

L
1
6
1
5





L-1615

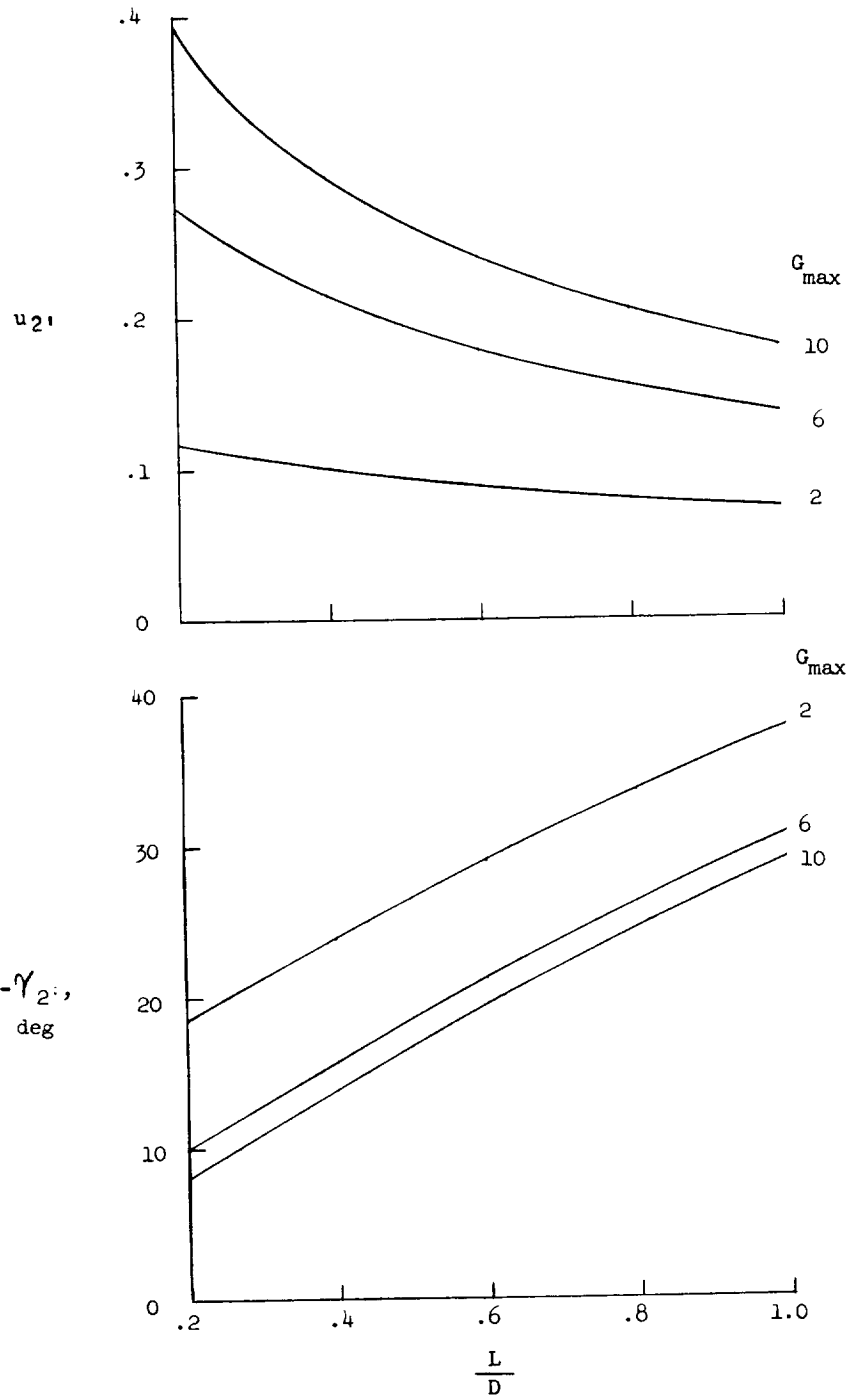


Figure 8.- Velocity and flight-path angle at the end of constant-G slow-up.

